1524 *Biochemistry* **2011,** *50,* 1524–1534
DOI: 10.1021/bi101240v

BIOCHEMISTRY
including biophysical chemistry & molecular biology
Article

Tyrosine Sulfation Influences the Chemokine Binding Selectivity of Peptides Derived from Chemokine Receptor CCR3[†]

John Z. Zhu,[‡] Christopher J. Millard,[§] Justin P. Ludeman,[§] Levi S. Simpson,[∥] Daniel J. Clayton,[§] Richard J. Payne,[⊥] Theodore S. Widlanski,[∥] and Martin J. Stone*[,§]

[‡]*Interdisciplinary Program in Biochemistry, Indiana University, Bloomington, Indiana 47405, United States ,* [§]*Department of Biochemistry and Molecular Biology, Monash University, Clayton, VIC 3800, Australia,* [∥]*Department of Chemistry, Indiana University, Bloomington, Indiana 47405, United States , and* [⊥]*School of Chemistry, Building F11, The University of Sydney, Sydney, NSW 2006, Australia*

Received August 3, 2010; Revised Manuscript Received January 13, 2011

ABSTRACT: The interactions of chemokines with their G protein-coupled receptors play critical roles in the control of leukocyte trafficking in normal homeostasis and in inflammatory responses. Tyrosine sulfation is a common post-translational modification in the amino-terminal regions of chemokine receptors. However, tyrosine sulfation of chemokine receptors is commonly incomplete or heterogeneous. To investigate the possibility that differential sulfation of two adjacent tyrosine residues could bias the responses of chemokine receptor CCR3 to different chemokines, we have studied the binding of three chemokines (eotaxin-1/CCL11, eotaxin-2/CCL24, and eotaxin-3/CCL26) to an N-terminal CCR3-derived peptide in each of its four possible sulfation states. Whereas the nonsulfated peptide binds to the three chemokines with approximately equal affinity, sulfation of Tyr-16 gives rise to 9−16-fold selectivity for eotaxin-1 over the other two chemokines. Subsequent sulfation of Tyr-17 contributes additively to the affinity for eotaxin-1 and eotaxin-2 but cooperatively to the affinity for eotaxin-3. The doubly sulfated peptide selectively binds to both eotaxin-1 and eotaxin-3 approximately 10-fold more tightly than to eotaxin-2. Nuclear magnetic resonance chemical shift mapping indicates that these variations in affinity probably result from only subtle differences in the chemokine surfaces interacting with these receptor peptides. These data support the proposal that variations in sulfation states or levels may regulate the responsiveness of chemokine receptors to their cognate chemokines.

Leukocyte trafficking in normal homeostasis as well as inflammatory responses is regulated, in part, by the interactions between chemokines and their receptors (*1*−*5*). Chemokines are small soluble proteins that are secreted from target tissues, whereas chemokine receptors are G protein-coupled receptors (GPCRs)[1] located in leukocyte membranes. Although numerous chemokine structures have been described, no structures of chemokine receptors have yet been reported. Nevertheless, studies of receptor mutants and chimeras have indicated that receptors interact with cognate chemokine ligands via the receptor extracellular elements and that, among these, the receptor amino-terminal element is critical for the initial binding of ligands (*6*−*10*).

Many receptors (and therefore the leukocytes expressing these receptors) respond to multiple chemokines. Regulation of these responses may occur at multiple levels (*5*), including receptor and ligand expression levels (*5*), localization of ligands by binding to glycosaminoglycans (*11*), proteolytic processing of chemokines (*12*, *13*), the presence of competing chemokines or other ligands (agonists or antagonists) (*5*), the presence of competing receptors on the same cell type or other cell types (including nonsignaling "decoy" receptors) (*14*, *15*), receptor oligomerization (*16*, *17*), receptor internalization and recycling (*18*), and intracellular signaling pathways (*19*). In addition, most, if not all, chemokine receptors are post-translationally sulfated on tyrosine residues in their amino-terminal elements, and sulfation enhances binding to chemokine ligands as well as pathogens (*20*−*24*).

Tyrosine sulfation is a common post-translational modification of secreted and cell-surface proteins that occurs in the trans-Golgi network, catalyzed by the enzymes tyrosylprotein sulfotransferase-1 and -2 (TPST-1 and -2, respectively) (*25*−*27*). Although labile to acid, sulfotyrosine is stable under normal physiological conditions, and in stark contrast to phosphorylation, there is currently no evidence that tyrosine sulfation is dynamically regulated. TPSTs are selective for tyrosine residues close in sequence to acidic amino acids, such as those in the amino-terminal elements of chemokine receptors (*28*). Mutation of tyrosine residues in the amino-terminal regions of receptors CCR5, CCR8, CXCR3, CXCR4, and CX_3CR1 and Duffy antigen and receptor for chemokines (DARC) has been shown to reduce the level of metabolic sulfate labeling of these receptors and the level of binding and/or activation of the receptors by

[†]This work was supported by Australian Research Council Grants DP DP0881570 and LE0989504 (to M.J.S.) and DP1094884 (to R.J.P. and M.J.S.) and by the Chester Davis Fellowship (to L.S.S.).

*To whom correspondence should be addressed: Department of Biochemistry and Molecular Biology, Monash University, Clayton, VIC 3800, Australia. Phone: +61-3-9902-9246. Fax: +61-3-9902-9500. E-mail: martin.stone@monash.edu.

[1]Abbreviations: $\Delta\delta_{NH}$, weighted change in the NH chemical shift; $\Delta\delta_{CH}$, weighted change in the CH chemical shift; DARC, Duffy antigen and receptor for chemokines; GPCR, G protein-coupled receptor; HSQC, heteronuclear single-quantum coherence spectrum; m_{NS}, slope of the nonsaturating binding phase; MR, molar ratio ([peptide]/[protein]); TPST, tyrosylprotein sulfotransferase.

 Published on Web 01/14/2011

cognate chemokines (*22*, *23*, *29*−*32*). Similarly, the chemokine binding affinities of amino-terminal peptides from receptors CCR3, CCR5, and CXCR4 are enhanced by sulfation of tyrosine residues in these peptides (*33*−*36*).

In addition to providing evidence of the presence of tyrosine sulfation, metabolic sulfate labeling studies indicate that the sulfation of certain tyrosine residues is incomplete (*22*, *23*). Thus, chemokine receptors may exist as heterogeneous mixtures of different sulfation states. In addition, the two TPST isoforms have different relative catalytic efficiencies for different target sequences (*37*, *38*), and both the total and relative expression levels of the two TPST isoforms vary substantially across different tissues (*27*). Consequently, it is likely that the levels of differently sulfated forms of chemokine receptors are dependent on the cell type in which the receptor is expressed and possibly also on environmental factors to which the cells are sensitive. This raises the intriguing possibility that variations in sulfation state could regulate the responsiveness of chemokine receptors to their cognate chemokines. Consistent with this possibility, Choe et al. observed that both Tyr-30 and Tyr-41 of DARC are sulfated, although probably not to completion, but that mutation of each tyrosine residue weakened binding to different chemokines (*23*).

CCR3 is a chemokine receptor expressed primarily on eosinophils, basophils, and Th2 cells (*39*). Chemokine activation of CCR3 plays a role in regulating leukocyte recruitment in allergic responses and parasitic infections (*39*−*42*). In addition, chemokine activation of CCR3 has recently been shown to stimulate choroidal neovascularization in a model of macular degeneration (*43*). The amino-terminal region of CCR3 contains two adjacent potential sulfation sites (Tyr-16 and Tyr-17), and this region can be sulfated when expressed as an immunoglobulin domain fusion protein, although sulfation of the intact receptor has not been described. We recently showed that sulfation of Tyr-17 of a CCR3-derived peptide enhances the affinity of this peptide for the chemokine eotaxin-1/CCL11 by a factor of 7, whereas sulfation of Tyr-16 enhances the affinity more than 28-fold (*33*). These results suggested that differential sulfation states of the receptor may respond differently to the same chemokine. Considering that CCR3 is also the target receptor for several other chemokines, these results further raised the possibility that sulfation of different tyrosine residues in CCR3 could bias the responses of the receptor to different chemokine ligands, thereby allowing regulation of chemokine selectivity through differences in sulfation state. As an initial test of this possibility, we describe herein an NMR study of the interactions of three CCR3 ligands (eotaxin-1/CCL11, eotaxin-2/CCL24, and eotaxin-3/CCL26) with an N-terminal CCR3 peptide in each of its four possible sulfation states.

EXPERIMENTAL PROCEDURES

Sulfopeptide Synthesis and Concentration Determination. Sulfopeptides were synthesized by solid-phase peptide synthesis using an Fmoc protection strategy, as described previously (*33*, *44*). Determination of the sulfopeptide concentration by UV absorbance is complicated by the fact that the absorbance at 280 nm (A_{280}) of sulfotyrosine is dramatically weaker than that of unmodified tyrosine and the absorbance maximum of sulfotyrosine is shifted to approximately 260 nm (*45*). Therefore, the concentration of peptide Su0 was determined using the calculated molar extinction coefficient at 280 nm (ε_{280} = 2560 cm^{-1} M^{-1}). The ε_{280} values of the singly sulfated peptides (Su16 and Su17) were then determined by comparison of A_{214} values for samples of Su0, Su16, and Su17, under the assumption that all three peptides have identical ε_{214} values. Using this approach, we obtained ε_{280} values of 1366 cm^{-1} M^{-1} for both Su16 and Su17, which compares well with the calculated value of 1280 cm^{-1} M^{-1} expected if the absorbance is completely dominated by the nonsulfated tyrosine residue in these peptides. In the case of Su1617, the absorbance at 280 nm was not significantly greater than baseline readings, so the absorbance at 260 nm was used to obtain initial estimates of Su1617 concentrations for NMR titrations; an ε_{260} value of 975 cm^{-1} M^{-1} was determined by comparison of A_{214} for samples of Su0 and Su1617. Subsequently, the concentrations of Su1617 used in NMR titrations were corrected (decreased by a factor of 2.0) on the basis of the stock solution concentration determined by amino acid analysis. Amino acid analysis was performed by the W. M. Keck Foundation Biotechnology Resource Laboratory at Yale University (New Haven, CT).

Expression and Purification of Chemokines. Eotaxin-1, -2, and -3 were expressed and purified using previously described methods (*46*−*48*). Briefly, each chemokine was expressed in *Escherichia coli* as a fusion protein containing an N-terminal His_6 tag, followed by a protease (thrombin or factor Xa) cleavage site, followed by the chemokine sequence. Eotaxin-1 was expressed as a soluble protein, whereas eotaxin-2 and eotaxin-3 were expressed in inclusion bodies. Uniform ^{15}N labeling was obtained by expression using ^{15}N-enriched M9 minimal medium (6 g/L Na_2HPO_4, 3 g/L KH_2PO_4, 0.5 g/L NaCl, 1 g/L $^{15}NH_4Cl$, 1 mg/L biotin, 1 mg/L thiamine-HCl, 4 g/L glucose, 0.49 g/L $MgSO_4$, 2 mL/L of 10% yeast extract, and 1 mL/L of 100 mM $CaCl_2$). All proteins were initially purified by Ni affinity chromatography. Eotaxin-2 and eotaxin-3 were then refolded. Subsequently, all proteins were subjected to protease cleavage and ion exchange chromatographic purification and characterized by SDS−PAGE, MALDI-TOF mass spectrometry, and NMR spectroscopy.

NMR Experiments and Assignments. NMR spectra were recorded on a Varian NMR Systems 600 MHz spectrometer equipped with a triple-resonance Cold Probe or a Bruker Avance 600 NMR instrument equipped with a triple-resonance cryoprobe. Chemical shifts were referenced to external 4,4-dimethyl-4-silapentane-1-sulfonic acid (DSS). Data were processed using NMRPipe (*49*), and spectral analyses were performed using Sparky (T. D. Goddard and D. G. Kneller, University of California, San Francisco, CA). Amide ^1H and ^{15}N NMR assignments of eotaxin-1, -2, and -3 under the conditions used for the peptide titrations (20 mM sodium acetate, 0.02% NaN_3, 10% D_2O, pH 6.5, 25 °C) were derived from previously published assignments. For eotaxin-1, the published assignments (*50*, *51*) could be used directly. For eotaxin-2 and eotaxin-3, previous assignments were made at pH 4.5 and 5.0, respectively (*47*, *48*); assignments at pH 6.5 were obtained by comparison of HSQC spectra recorded at pH increments of ~0.5 unit over the ranges 4.5−6.5 (for eotaxin-2) and 5.0−6.5 (for eotaxin-3). Amide ^1H and ^{15}N assignments for each protein under the conditions of the peptide titration experiments are listed in the Supporting Information. Backbone and side chain aliphatic CH groups were assigned under the conditions of the peptide binding experiments using a combination of two-dimensional (2D) $^{13}C-^1H$ HSQC and three-dimensional HNCACB, CBCA(CO)NH, H(CCCO)-NH, HCCH-TOCSY, and ^{15}N-separated TOCSY-HSQC experiments.

NMR Titrations of Eotaxin-1, -2, and -3 with Sulfopeptides. Titrations of ^{15}N-labeled eotaxin-1, -2, and -3 with synthetic peptides were performed using initial 50 μM samples containing eotaxin-1, -2, or -3 in NMR titration buffer [20 mM sodium acetate, 0.02% NaN_3, and 10% D_2O (pH 6.5)]. The peptide, in the same buffer, was added in several aliquots from a stock solution (1 mM for Su0, Su16, and Su17 and 500 μM for Su1617) to give final molar ratios (MR = [peptide]/[protein]) of 0.4, 0.8, 1.2, 1.6, 2, 2.5, 3.0, 4.0, and 5.0 for the titration of eotaxin-1, -2, and -3 with peptide Su0; 0.2, 0.4, 0.6, 0.8, 1.0, 1.2, 1.4, 2, 2.5, 3.5, and 5.0 for the titration of eotaxin-1, -2, and -3 with sulfopeptides Su16 and Su17; and 0.1, 0.2, 0.3, 0.4, 0.5, 0.6, 0.7, 1.0, 1.25, 1.75, and 2.5 for the titration of eotaxin-1, -2, and -3 with sulfopeptide Su1617. All titrations began with an initial volume of 500 μL and ended with a final volume of 625 μL. For the initial sample and after each addition, a gradient sensitivity-enhanced ^{15}N HSQC spectrum (*52*) was recorded at 25 °C using spectral widths of 2100 and 10000 Hz and 128 and 2048 complex data points in the ^{15}N and ^{1}H dimensions, respectively.

Analysis of Binding Data. For each point in each titration experiment, the ^{1}H and ^{15}N chemical shift values were determined for each observable amide resonance. The weighted change in chemical shift, relative to protein alone, was then calculated as $\Delta\delta_{NH} = |\Delta\delta_H| + 0.2|\Delta\delta_N|$. For each peptide to protein titration, the $\Delta\delta_{NH}$ values were then fit simultaneously, using OriginPro version 8, to the equation

$$\Delta\delta_{NH} = 0.5\Delta\delta_{NH,max,fit}\left(1 + MR + \frac{K_d}{C_e} - \sqrt{1 + MR + \frac{K_d}{C_e} - 4MR}\right) \quad (1)$$

where $\Delta\delta_{NH,max,fit}$ is the maximal change in weighted chemical shift (fit individually for each residue), K_d is the equilibrium dissociation constant (fit globally for all residues), MR is the molar ratio ([peptide]/[protein]) at each titration point, and C_e is the concentration of eotaxin-1, -2, or -3 at each titration point. Residues were included in the fitting only if their $\Delta\delta_{NH}$ values in the final point of the titration ($\Delta\delta_{NH,max}$) exceeded a designated cutoff value of 0.02 ppm for titration of Su0 into eotaxin-2 and 0.04 pm for all other titrations. For the titration of eotaxin-3 with sulfopeptide Su1617, the $\Delta\delta_{NH}$ data were fit simultaneously, using OriginPro version 8, using the two-phase binding equation

$$\Delta\delta_{NH} = 0.5\Delta\delta_{NH,max,fit}\left(1 + MR + \frac{K_d}{C_e} - \sqrt{1 + MR + \frac{K_d}{C_e} - 4MR}\right) + m_{NS}MR \quad (2)$$

where m_{NS} represents the slope of the nonsaturating component of the binding curve in the range of peptide concentrations used. Residues were included in the fitting only if their final $\Delta\delta_{NH}$ values exceeded 0.04 ppm. Considering that the initial concentration of chemokines in the binding experiments was 50 μM, K_d values much below ~5 μM cannot be determined precisely from binding curves for individual residues. However, the global fitting approach used herein allowed us to determine K_d values as low as ~1 μM with reasonable precision.

CH Chemical Shift Perturbations. The influence of peptide binding on specific CH group chemical shifts was assessed by recording ^{13}C−^{1}H HSQC spectra of each chemokine (20 μM) alone and in the presence of two different concentrations of each peptide, chosen on the basis of the K_d values to result in observably different levels of binding saturation. The following peptide concentrations were used: 80 and 200 μM for Su0 binding to all chemokines; 50 and 200 μM for Su16 binding to eotaxin-2 and eotaxin-3, Su17 binding to all chemokines, and Su1617 binding to eotaxin-2; and 10 and 50 μM for Su16 binding to eotaxin-1 and for Su1617 binding to eotaxin-1 and eotaxin-3. The degree of saturation for each experiment is listed in Table S4 of the Supporting Information. These spectra were recorded at 25 °C in 20 mM sodium acetate, 0.02% NaN_3, and 10% D_2O (pH 6.5). Weighted chemical shift changes for CH resonances were calculated as $\Delta\delta_{CH} = |\Delta\delta_H| + 0.25|\Delta\delta_C|$.

```
          8              16  17          23
Su0:      VETFGTTS    Y   Y  DDVGLL
Su16:     VETFGTTS   sY   Y  DDVGLL
Su17:     VETFGTTS    Y  sY  DDVGLL
Su1617:   VETFGTTS   sY  sY  DDVGLL
```

FIGURE 1: Sequences of the four peptides used in this study. Peptide names are shown at the left, and peptide sequences are given as one-letter amino acid codes (sY = sulfotyrosine). The numbering at the top corresponds to the amino acid position in receptor CCR3.

RESULTS

To investigate the role of site-specific tyrosine sulfation in chemokine binding, we studied chemokine binding by the four peptides shown in Figure 1. All four peptides have identical amino acid sequences corresponding to residues 8−23 of CCR3. The nonsulfated form of this peptide (Su0) was previously shown to bind to eotaxin-1 with affinity only slightly lower than that of the full-length N-terminal element of CCR3 (residues 1−35) (*46*). We compared the binding of the four peptides to each of three cognate chemokines for CCR3 (eotaxin-1, eotaxin-2, and eotaxin-3). Previous NMR studies of these three chemokines have been performed under a range of solution conditions (pH ranging from 4.0 to 6.5 and temperatures between 4.0 and 30 °C). We chose the conditions for the binding experiments reported herein (pH 6.5 and 25 °C) to be identical for all chemokines, to avoid acid-catalyzed hydrolysis of the sulfotyrosine moiety, and to provide sufficiently sharp NMR signals. Under these conditions, it was possible to observe resonances from most backbone NH groups in secondary structure regions, but many of the NH groups in the unstructured N-terminal and N-loop regions were not observable, presumably because of fast exchange with solvent.

Peptide Binding to Eotaxin-1. Binding of the four peptides to eotaxin-1 was assessed by monitoring changes in the ^{15}N−^{1}H correlation (HSQC) NMR spectrum of eotaxin-1 upon stepwise addition of each peptide. As an example, data for the amide resonance of residue Ala-51 are shown in Figure 2A. In general, chemical shift changes were more pronounced for the sulfated peptides than for peptide Su0. For Su0, only nine residues had weighted chemical shift changes exceeding 0.04 ppm after addition of 5 molar equiv of peptide ($\Delta\delta_{NH,max}$). However, for Su16, Su17, and Su1617, the corresponding numbers of residues were 23, 25, and 28, respectively. The $\Delta\delta_{NH,max}$ values for the four peptides and all observed protein residues are presented graphically in Figure 3A,D.

The equilibrium dissociation constant (K_d) of each peptide for eotaxin-1 was determined by globally fitting the $\Delta\delta_{NH}$ values as a function of peptide concentration. For all peptides, the data were consistent with a simple 1:1 binding interaction, and the data for all residues were fit well by a single global K_d value. Binding

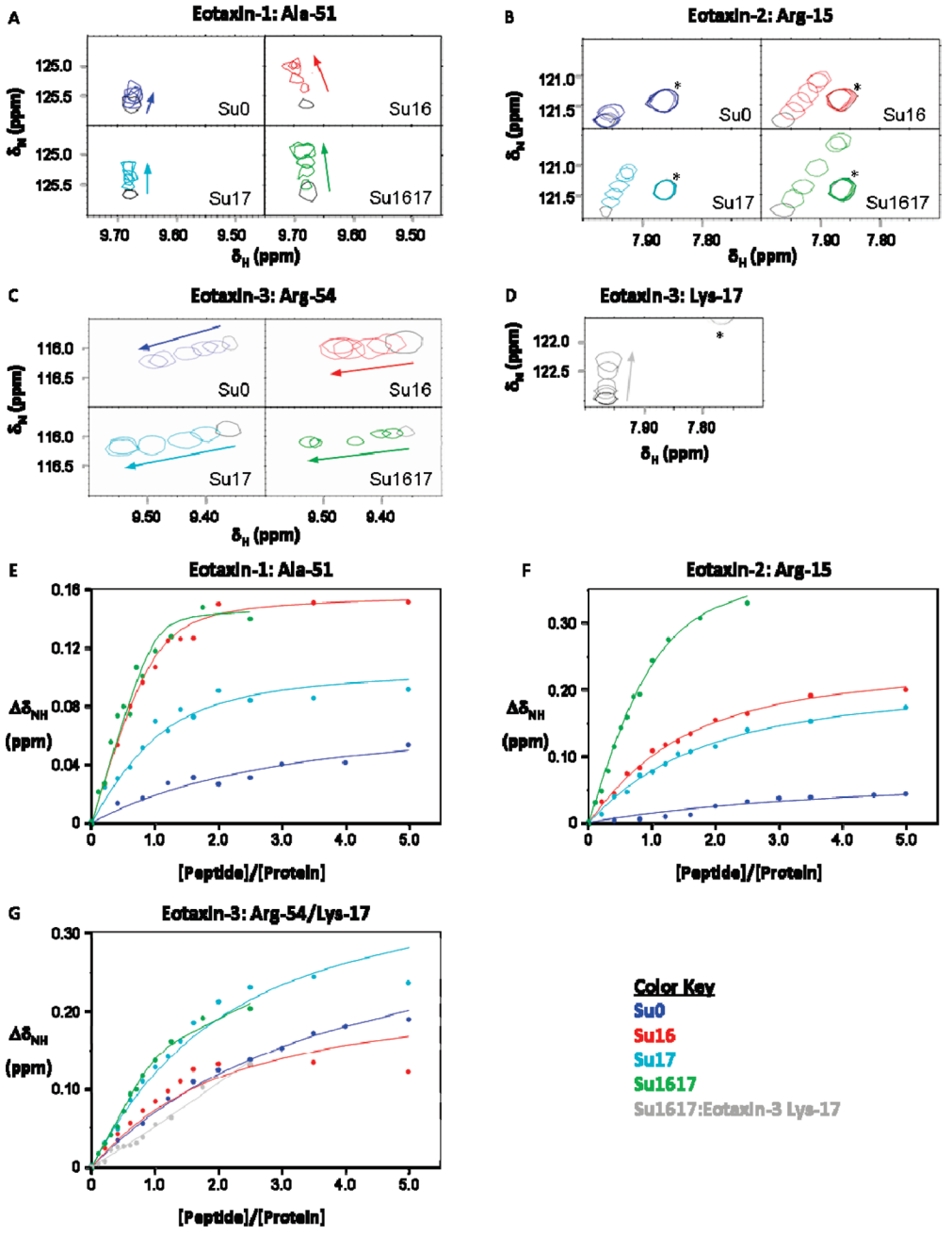

FIGURE 2: Binding data for interactions of CCR3-derived peptides with chemokines. (A−D) Expanded regions of the $^{1}H-^{15}N$ correlation (HSQC) spectra of (A) eotaxin-1, (B) eotaxin-2, and (C and D) eotaxin-3 containing the backbone amide peaks for (A) Ala-51, (B) Arg-15, (C) Val-49, and (D) Lys-17. In panels A−C, each region is shown in the absence of peptide (gray contour in each of the four panels) and in the presence of increasing concentrations of Su0 (blue contours), Su16 (red contours), Su17 (cyan contours), and Su1617 (green contours). In panel D, the Lys-17 peak is shown (gray) for increasing concentrations of Su1617. Arrows indicate the direction of peak movement. Asterisks indicate peaks that are present in the same region of the spectrum but do not shift in response to peptide binding. (E−G) Graphs showing the change in backbone $^{1}H_N$ chemical shift for (E) Ala-51 of eotaxin-1, (F) Arg-15 of eotaxin-2, and (G) Val-49 of eotaxin-3 as a function of the molar ratio of added peptide to chemokine. Uncertainties in $^{1}H_N$ chemical shifts are approximately 0.004 ppm. Solid lines represent the fitted binding curves obtained separately for each peptide by global analysis of all the binding data for that peptide (see the text for details). Data and fitted curves are colored for each peptide as in panels A−C. Panel G also shows the data and fitted curve for Lys-17 of eotaxin-3 upon binding to Su1617; Lys-17 undergoes only linear, nonsaturating changes in chemical shift.

isotherms are shown in Figure 2E and Figure S1 of the Supporting Information; the K_d values obtained are listed in Table 1. Whereas binding of Su0 was relatively weak ($K_d = 140 \pm 30\,\mu M$), sulfation of Tyr-16 or Tyr-17 enhanced affinity by factors of 7 and 28, respectively, whereas sulfation of both tyrosine residues enhanced affinity approximately 100-fold. The affinity values for the four peptides are the same, within error, as those we reported previously for the same binding interactions at a lower temperature (4 °C rather than 25 °C) (*33*).

Peptide Binding to Eotaxin-2. The interactions of CCR3 peptides with eotaxin-2 were also monitored using HSQC titrations. Examples of the spectral data and fitted binding curves are shown in panels B and F of Figure 2, respectively (see also Figure S2 of the Supporting Information); $\Delta\delta_{NH,max}$ values are presented in panels B and E of Figure 3, and fitted K_d values are listed in Table 1. The number of residues showing maximal chemical shift changes exceeding 0.04 ppm was somewhat smaller than that observed for eotaxin-1, but the sulfated peptides induced a

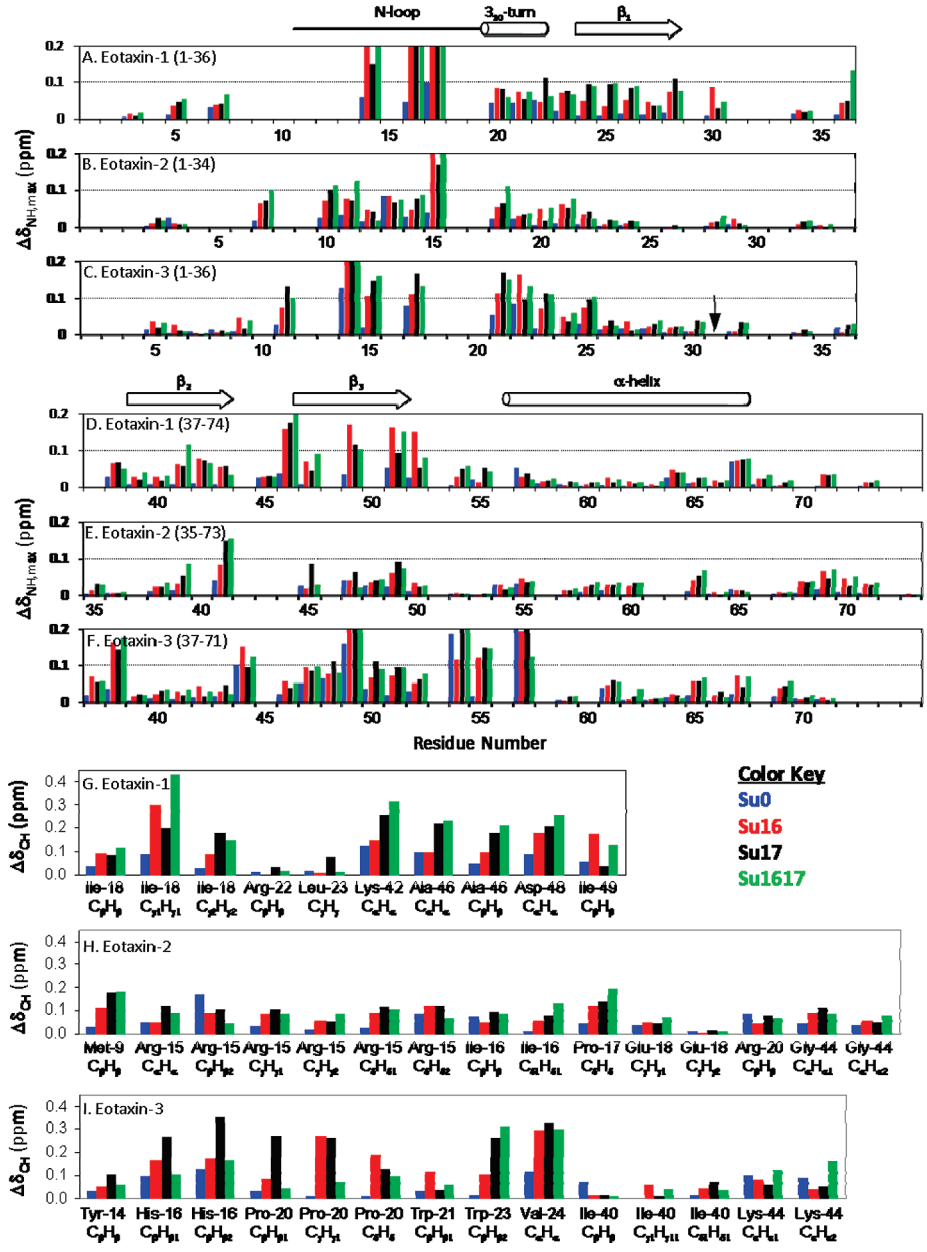

FIGURE 3: Chemokine chemical shift changes observed upon peptide binding. (A−F) Bar graphs showing the maximal changes in weighted amide chemical shift ($\Delta\delta_{NH,max}$) observed for specific residues of (A and D) eotaxin-1, (B and E) eotaxin-2, and (C and F) eotaxin-3 upon addition of Su0 (blue), Su16 (red), Su17 (black), and Su1617 (green). For the sake of clarity, the data for each chemokine are shown in two panels. Uncertainties in maximal shifts are approximately 0.004 ppm. Several residues exhibited $\Delta\delta_{NH,max}$ values exceeding 0.2 ppm (the maximum shown), as evident from the binding isotherms (Figure S1 of the Supporting Information). The residue numbers in each set of three panels (A−C and D−F) are aligned according to a structure-based sequence alignment of the three chemokines; the arrow in panel C denotes the position of a single-residue gap in the alignment for eotaxin-3. The consensus positions of secondary structure elements and the N-loop in the three chemokines are indicated schematically above panels A and D. (G−I) Bar graphs showing the weighted changes in CH chemical shift ($\Delta\delta_{CH}$) observed for specific resonances of (G) eotaxin-1, (H) eotaxin-2, and (I) eotaxin-3 upon addition of Su0 (blue), Su16 (red), Su17 (black), and Su1617 (green). Data are shown for resolved resonances assigned to CH groups in the N-loop and 3_{10}-turn and the $\beta2-\beta3$ hairpin for which significant changes in chemical shifts (i.e., changes exceeding the line width) were observed upon binding to one or more peptide(s); all shifts have been normalized to correct for the fraction of chemokine bound to peptide at the highest peptide concentration used (see Table S2 of the Supporting Information).

number of significant shifts (16 or 17 residues each) larger than the number observed for Su0 (only 3 residues). For all peptides, the data were consistent with a global 1:1 binding model, although the fits were of poorer quality for Su0 than for the other peptides because of the relatively weak shifts induced by the nonsulfated peptide. As for eotaxin-1, binding of Su0 was relatively weak (K_d = 240 ± 80 μM). Sulfation of Tyr-16 or Tyr-17 enhanced affinity by a factor of 5 or 4, respectively, and sulfation of both tyrosine residues enhanced affinity by a factor of 17.

Peptide Binding to Eotaxin-3. Binding of the four peptides to eotaxin-3 was also assessed using HSQC titrations. Examples of the spectral data are shown in panels C and D of Figure 2. Once again, Su0 induced changes in relatively few resonances ($\Delta\delta_{NH,max} \geq 0.04$ ppm for 11 residues), whereas the sulfated peptides induced changes in larger numbers of residues (28 or 29 each). The binding data for peptides Su0, Su16, and Su17 could be globally fit to a simple 1:1 binding model (Figure 2G). However, the data for Su1617 were not consistent with this simple model. Moreover, when the Su1617 binding data were fit

Table 1: Affinities of Chemokines for CCR3-Dervied Peptides and Native CCR3

	eotaxin-1	eotaxin-2	eotaxin-3
Su0[a] (μM)	140 ± 30	240 ± 80	200 ± 10
Su16[a] (μM)	5 ± 0.5	47 ± 4	78 ± 4
Su17[a] (μM)	20 ± 1	63 ± 5	85 ± 5
Su1617[a] (μM)	1.3 ± 0.3	14 ± 2	0.8 ± 0.6
CCR3[b] (nM)	2.1 ± 0.1	9.7 ± 0.8	1.2 ± 0.2

[a]Values shown for peptides are equilibrium dissociation constants (K_d) obtained by global fitting of the NMR titration data as described in Experimental Procedures. [b]Values shown for CCR3 are IC_{50} values obtained from competitive radioligand binding assays using CHO cells expressing CCR3 (*53*).

individually for each residue of eotaxin-3, the resulting K_d values varied over a wide range and the quality of the fits was often poor, suggesting that more than one binding event was occurring. Upon closer examination, we noticed that some resonances [e.g., Lys-17 (Figure 2D,G)] shifted linearly across the whole range of peptide concentrations without showing any evidence of saturation, whereas others [e.g., Val-49 (Figure 2C,G)] showed curves that resembled saturation binding superimposed on a linear, nonsaturating change in chemical shift. To account for the presence of nonsaturating binding, we fit the Su1617 binding data globally using a two-phase binding equation (see Experimental Procedures). This approach allowed us to determine a single K_d value describing the saturating phase of the binding, to identify the residues whose amide resonances are sensitive to the saturating phase of binding, and to obtain the $\Delta\delta_{NH}$ values for these residues at saturation ($\Delta\delta_{NH,max,fit}$). These data could then be compared directly to the K_d and $\Delta\delta_{NH,max}$ values observed for other peptide−chemokine pairs. In addition, this analysis identified the residues that are sensitive to the nonsaturating binding phase and yielded a slope for the nonsaturating part of each curve (m_{NS}), indicating the relative sensitivity of each residue to this component of the binding. Figure 2G shows examples of Su1617−eotaxin-3 titration data fit using the two-phase model, and Figure S3 of the Supporting Information shows a comparison of the global single-site and global two-phase fits for the 29 residues whose fitted $\Delta\delta_{NH,max}$ values exceed 0.04 ppm. The K_d values for binding of eotaxin-3 to all four peptides are listed in Table 1. Again, Su0 binds relatively weakly (K_d = 200 ± 10 μM). However, sulfation of individual tyrosine residues enhanced affinity by factors of 2−3, and sulfation of both tyrosine residues enhanced affinity by more than 2 orders of magnitude. The $\Delta\delta_{NH,max}$ values for binding of eotaxin-3 to each of the four peptides are compared in panels C and F of Figure 3. The fitted $\Delta\delta_{NH,max,fit}$ values for Su1617 are noticeably smaller than the experimental $\Delta\delta_{NH,max}$ values for Su16 and Su17, suggesting that fitting the data to the two-phase binding equation may underestimate these changes. Nevertheless, the pattern of changes is similar for all three sulfated peptides, allowing structural interpretation of the results.

Perturbation of CH Resonances by Peptide Binding. As discussed below, analysis of the backbone amide shift data suggested that the peptides interact primarily with the face of each chemokine defined by the N-loop and $\beta2-\beta3$ hairpin structural elements. To verify that these elements are involved in direct interactions with the peptides rather than undergoing indirect structural changes upon binding, we monitored the chemical shift changes of resolved CH groups in 2D $^{13}C-^{1}H$ HSQC spectra. For each chemokine, we identified 10−15 resolved CH resonances in the N-loop and $\beta2-\beta3$ hairpin that were sensitive to peptide binding. Examples of spectra illustrating these shifts are presented in Figure S4 of the Supporting Information, and bar graphs showing the shifts observed for each chemokine resonance and each peptide are presented in Figure 3G−I. Notably, for some residues, multiple side chain CH groups exhibited chemical shift perturbations, including Ile-18 of eotaxin-1; Arg-15, Ile-16, and Glu-18 of eotaxin-2; and His-16, Pro-20, Ile-40, and Lys-44 of eotaxin-3. A structural interpretation of the observed chemical shift changes is presented below.

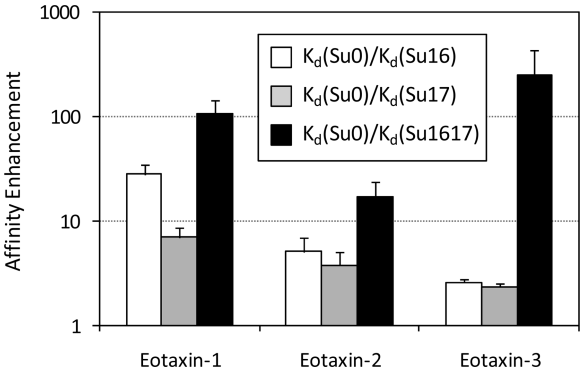

FIGURE 4: Enhancements of chemokine binding affinity induced by tyrosine sulfation at each position of the CCR3 peptide. The affinity enhancement upon Tyr-16 sulfation (white bars) is represented by the $K_d(Su0)/K_d(Su16)$ ratio; the affinity enhancement upon Tyr-17 sulfation (gray bars) is represented by the $K_d(Su0)/K_d(Su17)$ ratio, and the affinity enhancement upon sulfation of both tyrosine residues (black bars) is represented by the $K_d(Su0)/K_d(Su1617)$ ratio. The influence of sulfation at each position is additive for eotaxin-1 and eotaxin-2 but positively cooperative for eotaxin-3.

DISCUSSION

Sulfation Increases Chemokine Affinity Additively or Cooperatively. The affinity measurements in Table 1 indicate that sulfation of tyrosine residues in the N-terminal peptide of CCR3 increases the affinity of this peptide for cognate chemokines. Figure 4 shows the enhancements of affinity (ratios of equilibrium constants) for each chemokine that result from sulfation of Tyr-16, Tyr-17, or both Tyr residues. The data bars are presented on a logarithmic scale. Thus, if the Gibbs free energy contributions from sulfation at both Tyr-16 and Tyr-17 are independent, the data bars for double sulfation should be the sum of those for the two single-sulfation events (additive binding free energy). This situation is observed for both eotaxin-1 and eotaxin-2, although the K_d of Su1617 for eotaxin-1 was close to the lower limit of determination in our experiments. In contrast, for binding to eotaxin-3, the affinity enhancement observed for double sulfation is dramatically larger than the ~6-fold enhancement that would be expected if the two single-sulfation enhancements were additive, indicating positively cooperative binding contributions of the two sulfate groups. Thus, the data suggest that each sulfate group enhances the interaction of the other sulfate group with eotaxin-3 but not with the other two chemokines.

Sulfation Alters Chemokine Binding Selectivity. In addition to altering binding affinity, sulfation of tyrosine residues in the N-terminal peptide of CCR3 also changes the binding selectivity of this peptide for cognate chemokines. Although the nonsulfated peptide (Su0) binds to all three chemokines with

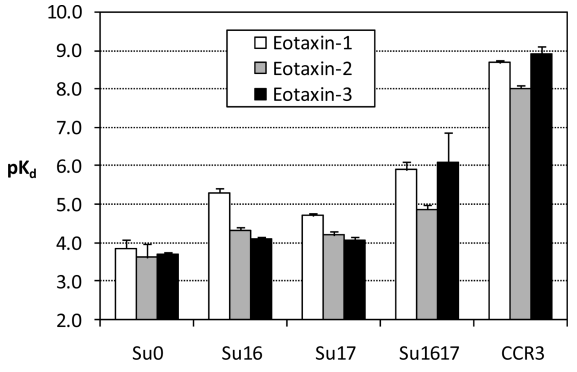

FIGURE 5: Selectivity of peptides and native CCR3 for the chemokines eotaxin-1, eotaxin-2, and eotaxin-3. Values shown are $pK_d = -\log(K_d)$ (K_d in molar) for eotaxin-1 (white bars), eotaxin-2 (gray bars), and eotaxin-3 (black bars). The K_d values for peptides Su0, Su16, Su17, and Su1617 were determined by NMR titration, whereas the K_d values for CCR3 are assumed to be equal to the IC_{50} values obtained from competitive radioligand binding assays using CHO cells expressing CCR3 (*53*).

similar affinities (Table 1), sulfation of Tyr-16 dramatically enhances the affinity for eotaxin-1 (by 28-fold) but provides only modest enhancements of affinity (3−5-fold) for the two other chemokines. Sulfation of Tyr-17 provides a much lower level of discrimination, with enhancements of 7-, 4-, and 2-fold for eotaxin-1, -2, and -3, respectively. These results indicate that addition of a single sulfate group to either Tyr residue of Su0 gives rise to binding selectivity in favor of eotaxin-1. In contrast, the addition of a second sulfate group to Su16 (i.e., conversion of Su16 to Su1617) yields a dramatic (approximately 80-fold) enhancement in affinity for eotaxin-3 but much smaller (3−4-fold) enhancements in affinity for eotaxin-1 or eotaxin-2.

The differential effects of the first and second sulfation events give rise to a distinct spectrum of selectivity for each form of the receptor peptide, as illustrated by the groups of data bars in Figure 5. Whereas the unsulfated peptide does not differentiate between the three ligands, Su16 strongly favors binding to eotaxin-1 over the other two chemokines (by 9- or 15-fold), Su17 weakly favors binding to eotaxin-1 over the other two chemokines (by 3- or 4-fold), and the doubly sulfated peptide favors binding to eotaxin-1 and eotaxin-3 over eotaxin-2 by approximately 1 order of magnitude. These results support the possibility that tyrosine sulfation is a mechanism for regulating the sensitivity of CCR3 to its various cognate chemokines.

The observation that tyrosine sulfation influences the chemokine binding selectivity of CCR3-derived peptides suggests that it is also likely to influence the selectivity of the intact receptor. Although there are no reports to date demonstrating sulfation of intact CCR3, Liu et al. (*28*) have used bioinformatic methods to predict that both Tyr-16 and Tyr-17 of CCR3 are more likely than not to be sulfated. In addition, the N-terminal region of CCR3 has been shown to undergo sulfation when expressed in HeLa cells as a fusion to the Fc domain of immunoglobulin IgG1 (*20*) and to be sulfated in vitro in the presence of recombinant TPST-1 or TPST-2 (*37*). Moreover, the relative affinities of eotaxin-1, -2, and -3 for CCR3 expressed on CHO cells (*53*) closely parallel the relative affinities of the same three chemokines for Su1617 (Figure 5), suggesting that the predominant form of CCR3 in these cells may be the form that is sulfated on both tyrosine residues.

Possible Structural Basis of Selectivity. The chemokine chemical shift changes induced by peptide binding provide an indication of the regions of the chemokines that interact with the CCR3-derived peptides. Numerous previous studies have shown that N-terminal peptides from chemokine receptors bind to cognate chemokines in the vicinity of a shallow crevice defined by the N-loop and $\beta2-\beta3$ hairpin structural elements (*34*, *35*, *46*, *48*, *54*, *55*). We refer to this surface as the "front face" of the chemokine. In this study, we found that the majority of residues undergoing amide chemical shift perturbations upon binding to CCR3 peptides are located on the front faces of the three chemokines, with relatively few chemical shift changes on the back face (Figure S6 of the Supporting Information). Furthermore, the perturbations observed for peptides Su0, Su16, and Su17 are generally a subset of those observed for Su1617 (Figure S5 of the Supporting Information). Therefore, we focus our discussion on the effects of Su1617 binding on the front faces of the chemokines.

Panels A and B of Figure 6 show the front faces of eotaxin-1, -2, and -3, indicating the residues that undergo amide chemical shift perturbations upon binding to peptide Su1617. For eotaxin-1, there are large perturbations in both the N-loop and the $\beta2-\beta3$ hairpin (red on the front face in panels A and B of Figure 6), and several perturbed residues [Arg-16, Lys-17, and Lys-47 (labeled in Figure 6B)] contribute substantially to a strongly basic region of the surface (intense blue in Figure 6C). The pattern of perturbations for eotaxin-2 is quite different from that observed for eotaxin-1. The highest concentration of perturbed residues is in the N-terminal, and central parts of the N-loop, including surface residues Phe-10, Ser-13, Lys-14, and Arg-15. The corresponding residues in eotaxin-1 are Asn-12, Asn-15, Arg-16, and Lys-17, respectively. Thus, the replacement of a small polar residue (Asn-12) in eotaxin-1 with a large hydrophobic residue (Phe-10) in eotaxin-2 and the replacement of Arg-16 and Lys-17 with Lys-14 and Arg-15, respectively, may give rise to a different binding position for the sulfopeptide on the chemokine surface. Interpretation of the amide chemical shift perturbations of eotaxin-3 is more difficult because of the two phases of binding observed with this chemokine. Nevertheless, the chemical shift perturbations for the saturating component of the binding are again on the front face of the chemokine, with no significant changes occurring on the back face (Figure S6 of the Supporting Information). For this chemokine, the major perturbations do not form a continuous surface but instead are localized to several patches, including Tyr-14, Ser-15, and Val-49 at the N-loop$-\beta3$ interface, Arg-54 and Trp-57 at the beginning of the α-helix, and Trp-21, Thr-22, and Lys-44 at the interface between the 3_{10}-turn and the $\beta2-\beta3$ hairpin; these elements are labeled in Figure 6A.

Many of the eotaxin-3 residues that are sensitive to the saturating phase of binding also display sensitivity to the nonsaturating phase of binding (Figure S6 of the Supporting Information). The nonsaturating component also affects several other residues, including some on the back face of the molecule. Many of the residues showing the largest m_{NS} values are adjacent to either two surface-exposed histidine residues (His-16 and His-52) or two surface-exposed tryptophan residues (Trp-21 and Trp-23), none of which is conserved in eotaxin-1 or eotaxin-2. We suggest that the nonsaturating component of binding may result from nonspecific interactions between the peptide and these histidine and/or tryptophan residues. Considering that the titration experiments were conducted at pH 6.5, changes in the ionization states of the histidine side chains could contribute to these interactions. Moreover, the proximity of these residues to the residues that are sensitive to the saturating component of

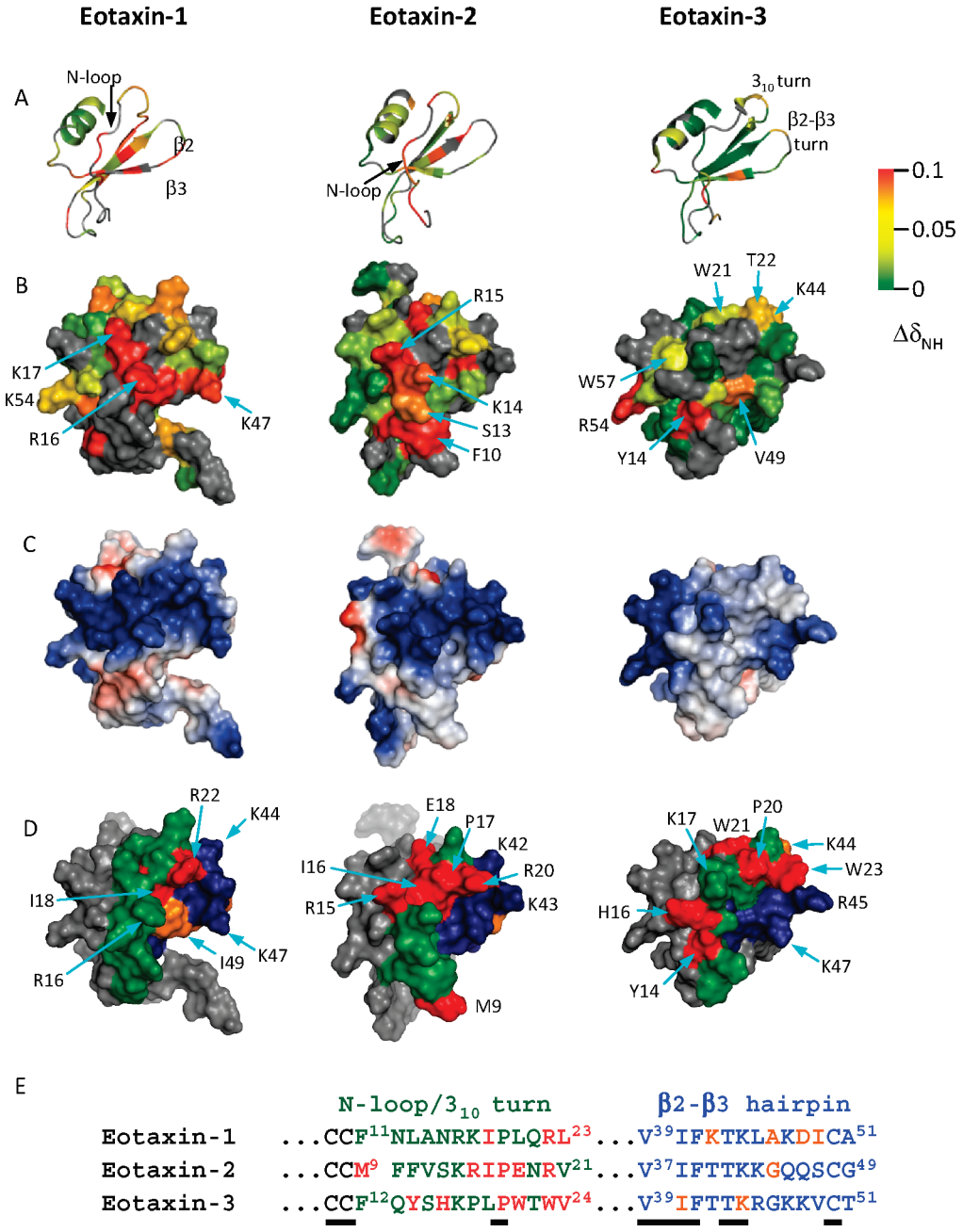

FIGURE 6: Structures of chemokines color-coded to show peptide binding. Shown are "front" views of the structures of eotaxin-1, eotaxin-2, and eotaxin-3 (Protein Data Bank entries 1EOT, 1EIG, and 1G2S, respectively). (A) Ribbon diagrams and (B) surface representations are color-coded according to the maximal change in weighted amide chemical shift ($\Delta\delta_{NH,max}$) upon binding of the indicated chemokines to Su1617. For eotaxin-1 and eotaxin-2, $\Delta\delta_{NH,max}$ values are those measured at the final point of the titration, whereas for eotaxin-3, they are those obtained by fitting to the two-phase binding model. (C) Surface representations of the chemokines color-coded according to electrostatic potential (blue, positive; red, negative). (D) Surface representations showing the N-loop and 3_{10}-turn (blue) and the $\beta2-\beta3$ hairpin (green) and highlighting residues within these two regions for which CH group shifts were observed (red for N-loop and 3_{10}-turn residues and orange for $\beta2-\beta3$ hairpin residues). For the sake of clarity, the ribbon diagrams (A) show only the ordered regions of the chemokines (eotaxin-1 residues 9−65, eotaxin-2 residues 7−63, and eotaxin-3 residues 10−65), whereas the surface representations in all the other panels include the disordered N- and C-terminal regions. Labeled residues and structural elements are discussed in the text. (E) Alignment of the N-loop, 3_{10}-turn, and $\beta2-\beta3$ hairpin sequences of eotaxin-1, -2, and -3, with residues color-coded as in panel D. Residue numbers are given for the first and last residue of each region. The CC motif, which immediately precedes the N-loop, is also shown (black). Black bars at the bottom indicate residues that are conserved among these three chemokines.

binding suggests that the two binding components may not be completely independent. We note that an alternative explanation for the second phase of peptide binding is that the binding could be coupled to dimerization of eotaxin-3, as observed previously for binding of a CXCR4 peptide to the chemokine SDF-1/CXCL12 (*35*). However, eotaxin-3 has not been observed to dimerize, even at concentrations of ~2 mM (*47*), and we have found no evidence (e.g., peak splitting or line broadening) to suggest dimerization of eotaxin-3 in this study. Therefore, this explanation remains speculative.

Amide chemical shift changes in NMR spectra can result from either direct binding interactions or indirect structural changes. In a previous study of the chemokine interleukin-8/CXCL8 binding to a CXCR1 peptide, amide shifts in the N-loop were

attributed to direct interactions whereas those in the β3 strand and the C-terminal α-helix were attributed to indirect structural adjustments (*56*). On the other hand, changes in side chain chemical shifts can be more confidently attributed to direct binding interactions. Therefore, we used $^{13}C-^{1}H$ correlation spectra to identify CH groups influenced by peptide binding. As this analysis relies on the presence of resolved CH resonances in crowded 2D spectra, it should not be expected to yield a complete map of the interaction surface but will instead help to validate the involvement of specific residues. Despite this limitation, we identified numerous CH groups in the N-loop, 3_{10}-turn, and $\beta2-\beta3$ hairpin of each chemokine that are sensitive to peptide binding. These are highlighted in Figure 6D and match well with the binding regions deduced from the amide chemical shift data. The data support the proposal that the N-terminus of CCR3 interacts with the same structural elements of each chemokine but that the specific residues involved in the interactions differ substantially. In this light, it is noteworthy that the sequences of the N-loop, 3_{10}-turn, and $\beta2-\beta3$ hairpin regions differ dramatically among the three chemokines (Figure 6E and Figure S7 of the Supporting Information). In particular, it is likely that differences in the positions of lysine and arginine residues in these regions result in different optimal positions of the sulfated peptides on the chemokine surfaces, although the overall basicities of the three chemokines are similar; all three have predicted isoelectric points in the range of 10.0 ± 0.2 and are predicted to have net charges of $+11$ to $+13$ under the conditions used in this study.

In a previous study of a CXCR4 peptide binding to SDF-1, comparison of the shifts for the singly sulfated and nonsulfated peptides (i.e., secondary shift analysis) indicated the likely binding position of the sulfate group in the sulfotyrosine residue, which was later verified by NMR structure determination (*34*, *35*). Similar analyses of the NH and CH chemical shift data presented here for nonsulfated versus singly sulfated peptides and for singly sulfated versus doubly sulfated peptides (Figures S8 and S9 of the Supporting Information) showed substantial secondary shifts for residues in the N-loop, 3_{10}-turn, and $\beta2-\beta3$ hairpin regions, providing further evidence that these regions are involved in binding to the sulfotyrosine residues. In general, the largest secondary shifts were observed for groups in the proximity of the positively charged residues in the N-loops of the chemokines, again supporting the above suggestions that the side chains of these residues interact with the sulfate groups. Nevertheless, precise identification of the sulfate binding sites will require detailed structure determination.

To date, the only structures determined for the interactions of sulfated chemokine receptor peptides with chemokines are the structures of the 38-residue CXCR4 N-terminus bound to chemokine SDF-1 (*34*, *35*, *46*, *48*, *54*, *55*). Structures were determined for nonsulfated, Y21-sulfated, and triply sulfated (Y7, Y12, and Y21) forms of the peptide bound to a cross-linked dimeric form of SDF-1; each chemokine dimer binds to two peptide molecules in a symmetric fashion. In these structures, Tyr-21 binds in the crevice between the N-loop and the β3 strand, the site equivalent to that suggested by our data for binding of CCR3 sulfated peptides to eotaxin-1, -2, and -3. However, the long CXCR4 peptide also wraps around the structure and spans the dimer interface, allowing Tyr-12 to interact with residues on the exposed face of the β-sheet (in the same monomer as the Tyr-21 binding site) and Tyr-7 to interact with residues in the 3_{10}-turn and the α-helix of the other monomer. Considering that the only sulfotyrosine residues in the N-terminus of CCR3 are residues 16 and 17, CCR3 does not have the potential to form the same types of interactions observed for CXCR4. However, the interaction of a sulfotyrosine residue with the N-loop and β3 region is a common feature that may be general to many chemokine−receptor interactions.

CONCLUDING REMARKS

We have demonstrated that sulfation of a peptide derived from CCR3 alters the selectivity of binding to cognate chemokines of CCR3. Although the sulfated peptides appear to interact predominantly with the same surface of the three chemokines, the specific amino acid residues involved in these interactions clearly differ between the chemokines. These different interactions may account for the substantially different influences of sulfation on binding to each chemokine. The results presented lend support to the notion that distinct patterns of tyrosine sulfation could influence the responsiveness of chemokine receptors to different chemokine ligands in vivo. Thus, they provide motivation for future studies aimed at characterizing the sulfation states of chemokine receptors.

ACKNOWLEDGMENT

We thank Richard DiMarchi and David Smiley at Indiana University and Patrick Perlmutter and Mibel Aguilar at Monash University for providing helpful advice and access to the peptide synthesizer, Nick Grossoehme for helpful discussions, and Douglas E. Brown, Xinfeng Gao, John W. Tomaszewski, and Peter Nichols for assistance with NMR spectroscopy.

SUPPORTING INFORMATION AVAILABLE

Tables of amide ^{1}H and ^{15}N assignments for eotaxin-1, eotaxin-2, and eotaxin-3 under the conditions of the peptide titrations; tables of peptide concentrations and degrees of saturation for $^{13}C-^{1}H$ HSQC experiments; binding isotherms and curve fits for binding of eotaxin-1, eotaxin-2, and eotaxin-3 to peptides Su0, Su16, Su17, and Su1617; regions of $^{13}C-^{1}H$ HSQC spectra showing chemokine resonances that shift in response to peptide binding; structures of eotaxin-1, eotaxin-2, and eotaxin-3 color-coded to indicate residues whose NH group NMR resonances shift upon binding to Su0, Su16, Su17, and Su1617; sequence alignment of eotaxin-1, eotaxin-2, and eotaxin-3, and results of secondary chemical shift analysis. This material is available free of charge via the Internet at http://pubs.acs.org.

NOTE ADDED IN PROOF

Since the original submission of this manuscript, the crystal structure of inhibitor-bound chemokine receptor CXCR4 has been reported (*57*). However, there are still no reported structures of chemokine receptors bound to chemokines.

REFERENCES

1. Zlotnik, A., and Yoshie, O. (2000) Chemokines: A new classification system and their role in immunity. *Immunity 12*, 121–127.
2. Thelen, M. (2001) Dancing to the tune of chemokines. *Nat. Immunol. 2*, 129–134.
3. Gerard, C., and Rollins, B. J. (2001) Chemokines and disease. *Nat. Immunol. 2*, 108–115.
4. Baggiolini, M. (2001) Chemokines in pathology and medicine. *J. Intern. Med. 250*, 91–104.
5. Moser, B., Wolf, M., Walz, A., and Loetscher, P. (2004) Chemokines: Multiple levels of leukocyte migration control. *Trends Immunol. 25*, 75–84.

6. Pease, J. E., Wang, J., Ponath, P. D., and Murphy, P. M. (1998) The N-terminal extracellular segments of the chemokine receptors CCR1 and CCR3 are determinants for MIP-1α and eotaxin binding, respectively, but a second domain is essential for efficient receptor activation. *J. Biol. Chem. 273*, 19972–19976.
7. Wu, L. J., Larosa, G., Kassam, N., Gordon, C. J., Heath, H., Ruffing, N., Chen, H., Humblias, J., Samson, M., Parmentier, M., Moore, J. P., and Mackay, C. R. (1997) Interaction of chemokine receptor CCR5 with its ligands: Multiple domains for HIV-1 gp120 binding and a single domain for chemokine binding. *J. Exp. Med. 186*, 1373–1381.
8. Xanthou, G., Williams, T. J., and Pease, J. E. (2003) Molecular characterization of the chemokine receptor CXCR3: Evidence for the involvement of distinct extracellular domains in a multi-step model of ligand binding and receptor activation. *Eur. J. Immunol. 33*, 2927–2936.
9. Hebert, C. A., Chuntharapai, A., Smith, M., Colby, T., Kim, J., and Horuk, R. (1993) Partial functional mapping of the human interleukin-8 type A receptor. Identification of a major ligand binding domain. *J. Biol. Chem. 268*, 18549–18553.
10. Leong, S. R., Kabakoff, R. C., and Hebert, C. A. (1994) Complete mutagenesis of the extracellular domain of interleukin-8 (IL-8) type A receptor identifies charged residues mediating IL-8 binding and signal transduction. *J. Biol. Chem. 269*, 19343–19348.
11. Proudfoot, A. E. I., Handel, T. M., Johnson, Z., Lau, E. K., LiWang, P., Clark-Lewis, I., Borlat, F., Wells, T. N. C., and Kosco-Vilbois, M. H. (2003) Glycosaminoglycan binding and oligomerization are essential for the in vivo activity of certain chemokines. *Proc. Natl. Acad. Sci. U.S.A. 100*, 1885–1890.
12. Richter, R., Casarosa, P., Standker, L., Munch, J., Springael, J. Y., Nijmeijer, S., Forssmann, W. G., Vischer, H. F., Vakili, J., Detheux, M., Parmentier, M., Leurs, R., and Smit, M. J. (2009) Significance of N-terminal proteolysis of CCL14a to activity on the chemokine receptors CCR1 and CCR5 and the human cytomegalovirus-encoded chemokine receptor US28. *J. Immunol. 183*, 1229–1237.
13. Savino, B., Borroni, E. M., Torres, N. M., Proost, P., Struyf, S., Mortier, A., Mantovani, A., Locati, M., and Bonecchi, R. (2009) Recognition versus adaptive up-regulation and degradation of CC chemokines by the chemokine decoy receptor D6 are determined by their N-terminal sequence. *J. Biol. Chem. 284*, 26207–26215.
14. Comerford, I., Litchfield, W., Harata-Lee, Y., Nibbs, R. J., and McColl, S. R. (2007) Regulation of chemotactic networks by 'atypical' receptors. *BioEssays 29*, 237–247.
15. Graham, G. J. (2009) D6 and the atypical chemokine receptor family: Novel regulators of immune and inflammatory processes. *Eur. J. Immunol. 39*, 342–351.
16. Akekawatchai, C., Holland, J. D., Kochetkova, M., Wallace, J. C., and McColl, S. R. (2005) Transactivation of CXCR4 by the insulin-like growth factor-1 receptor (IGF-1R) in human MDA-MB-231 breast cancer epithelial cells. *J. Biol. Chem. 280*, 39701–39708.
17. Salanga, C. L., O'Hayre, M., and Handel, T. (2009) Modulation of chemokine receptor activity through dimerization and crosstalk. *Cell. Mol. Life Sci. 66*, 1370–1386.
18. Neel, N. F., Schutyser, E., Sai, J., Fan, G. H., and Richmond, A. (2005) Chemokine receptor internalization and intracellular trafficking. *Cytokine Growth Factor Rev. 16*, 637–658.
19. Pribila, J. T., and Shimizu, Y. (2003) Signal transduction events regulating integrin function and T cell migration: New functions and complexity. *Immunol. Res. 27*, 107–128.
20. Farzan, M., Mirzabekov, T., Kolchinsky, P., Wyatt, R., Cayabyab, M., Gerard, N. P., Gerard, C., Sodroski, J., and Choe, H. (1999) Tyrosine sulfation of the amino terminus of CCR5 facilitates HIV-1 entry. *Cell 96*, 667–676.
21. Farzan, M., Vasilieva, N., Schnitzler, C. E., Chung, S., Robinson, J., Gerard, N. P., Gerard, C., Choe, H., and Sodroski, J. (2000) A tyrosine-sulfated peptide based on the N terminus of CCR5 interacts with a CD4-enhanced epitope of the HIV-1 gp120 envelope glycoprotein and inhibits HIV-1 entry. *J. Biol. Chem. 275*, 33516–33521.
22. Farzan, M., Babcock, G. J., Vasilieva, N., Wright, P. L., Kiprilov, E., Mirzabekov, T., and Choe, H. (2002) The role of post-translational modifications of the CXCR4 amino terminus in stromal-derived factor 1α association and HIV-1 entry. *J. Biol. Chem. 277*, 29484–29489.
23. Choe, H., Moore, M. J., Owens, C. M., Wright, P. L., Vasilieva, N., Li, W., Singh, A. P., Shakri, R., Chitnis, C. E., and Farzan, M. (2005) Sulphated tyrosines mediate association of chemokines and *Plasmodium vivax* Duffy binding protein with the Duffy antigen/receptor for chemokines (DARC). *Mol. Microbiol. 55*, 1413–1422.
24. Preobrazhensky, A. A., Dragan, S., Kawano, T., Gavrilin, M. A., Gulina, I. V., Chakravarty, L., and Kolattukudy, P. E. (2000) Monocyte chemotactic protein-1 receptor CCR2B is a glycoprotein that has tyrosine sulfation in a conserved extracellular N-terminal region. *J. Immunol. 165*, 5295–5303.
25. Kehoe, J. W., and Bertozzi, C. R. (2000) Tyrosine sulfation: A modulator of extracellular protein-protein interactions. *Chem. Biol. 7*, R57–R61.
26. Seibert, C., and Sakmar, T. P. (2008) Toward a framework for sulfoproteomics: Synthesis and characterization of sulfotyrosine-containing peptides. *Biopolymers 90*, 459–477.
27. Stone, M. J., Chuang, S., Hou, X., Shoham, M., and Zhu, J. Z. (2009) Tyrosine sulfation: An increasingly recognised post-translational modification of secreted proteins. *Nat. Biotechnol. 25*, 299–317.
28. Liu, J., Louie, S., Hsu, W., Yu, K. M., Nicholas, H. B., Jr., and Rosenquist, G. L. (2008) Tyrosine sulfation is prevalent in human chemokine receptors important in lung disease. *Am. J. Respir. Cell Mol. Biol. 38*, 738–743.
29. Gutierrez, J., Kremer, L., Zaballos, A., Goya, I., Martinez, A. C., and Marquez, G. (2004) Analysis of post-translational CCR8 modifications and their influence on receptor activity. *J. Biol. Chem. 279*, 14726–14733.
30. Colvin, R. A., Campanella, G. S., Manice, L. A., and Luster, A. D. (2006) CXCR3 requires tyrosine sulfation for ligand binding and a second extracellular loop arginine residue for ligand-induced chemotaxis. *Mol. Cell. Biol. 26*, 5838–5849.
31. Fong, A. M., Alam, S. M., Imai, T., Haribabu, B., and Patel, D. D. (2002) CX3CR1 tyrosine sulfation enhances fractalkine-induced cell adhesion. *J. Biol. Chem. 277*, 19418–19423.
32. Seibert, C., Cadene, M., Sanfiz, A., Chait, B. T., and Sakmar, T. P. (2002) Tyrosine sulfation of CCR5 N-terminal peptide by tyrosylprotein sulfotransferases 1 and 2 follows a discrete pattern and temporal sequence. *Proc. Natl. Acad. Sci. U.S.A. 99*, 11031–11036.
33. Simpson, L. S., Zhu, J. Z., Widlanski, T. S., and Stone, M. J. (2009) Regulation of chemokine recognition by site-specific tyrosine sulfation of receptor peptides. *Chem. Biol. 16*, 153–161.
34. Veldkamp, C. T., Seibert, C., Peterson, F. C., De la Cruz, N. B., Haugner, J. C., III, Basnet, H., Sakmar, T. P., and Volkman, B. F. (2008) Structural basis of CXCR4 sulfotyrosine recognition by the chemokine SDF-1/CXCL12. *Sci. Signaling 1*, ra4.
35. Veldkamp, C. T., Seibert, C., Peterson, F. C., Sakmar, T. P., and Volkman, B. F. (2006) Recognition of a CXCR4 sulfotyrosine by the chemokine stromal cell-derived factor-1α (SDF-1α/CXCL12). *J. Mol. Biol. 359*, 1400–1409.
36. Duma, L., Haussinger, D., Rogowski, M., Lusso, P., and Grzesiek, S. (2007) Recognition of RANTES by extracellular parts of the CCR5 receptor. *J. Mol. Biol. 365*, 1063–1075.
37. Mishiro, E., Sakakibara, Y., Liu, M. C., and Suiko, M. (2006) Differential enzymatic characteristics and tissue-specific expression of human TPST-1 and TPST-2. *J. Biochem. 140*, 731–737.
38. Danan, L. M., Yu, Z., Hoffhines, A. J., Moore, K. L., and Leary, J. A. (2008) Mass spectrometric kinetic analysis of human tyrosylprotein sulfotransferase-1 and -2. *J. Am. Soc. Mass Spectrom. 19*, 1459–1466.
39. Yawalkar, N., Uguccioni, M., Scharer, J., Braunwalder, J., Karlen, S., Dewald, B., Braathen, L. R., and Baggiolini, M. (1999) Enhanced expression of eotaxin and CCR3 in atopic dermatitis. *J. Invest. Dermatol. 113*, 43–48.
40. Jose, P. J., Adcock, I. M., Griffiths-Johnson, D. A., Berkman, N., Wells, T. N., Williams, T. J., and Power, C. A. (1994) Eotaxin: Cloning of an eosinophil chemoattractant cytokine and increased mRNA expression in allergen-challenged guinea-pig lungs. *Biochem. Biophys. Res. Commun. 205*, 788–794.
41. Jose, P. J., Griffiths-Johnson, D. A., Collins, P. D., Walsh, D. T., Moqbel, R., Totty, N. F., Truong, O., Hsuan, J. J., and Williams, T. J. (1994) Eotaxin: A potent eosinophil chemoattractant cytokine detected in a guinea pig model of allergic airways inflammation. *J. Exp. Med. 179*, 881–887.
42. Rankin, S. M., Conroy, D. M., and Williams, T. J. (2000) Eotaxin and eosinophil recruitment: Implications for human disease. *Mol. Med. Today 6*, 20–27.
43. Takeda, A., Baffi, J. Z., Kleinman, M. E., Cho, W. G., Nozaki, M., Yamada, K., Kaneko, H., Albuquerque, R. J., Dridi, S., Saito, K., Raisler, B. J., Budd, S. J., Geisen, P., Munitz, A., Ambati, B. K., Green, M. G., Ishibashi, T., Wright, J. D., Humbles, A. A., Gerard, C. J., Ogura, Y., Pan, Y., Smith, J. R., Grisanti, S., Hartnett, M. E., Rothenberg, M. E., and Ambati, J. (2009) CCR3 is a target for age-related macular degeneration diagnosis and therapy. *Nature 460*, 225–230.
44. Simpson, L. S., and Widlanski, T. S. (2006) A comprehensive approach to the synthesis of sulfate esters. *J. Am. Chem. Soc. 128*, 1605–1610.
45. Ward, C. M., Andrews, R. K., Smith, A. I., and Berndt, M. C. (1996) Mocarhagin, a novel cobra venom metalloproteinase, cleaves the

platelet von Willebrand factor receptor glycoprotein Ibα. Identification of the sulfated tyrosine/anionic sequence Tyr-276-Glu-282 of glycoprotein Ibα as a binding site for von Willebrand factor and α-thrombin. *Biochemistry 35*, 4929–4938.
46. Ye, J., Kohli, L. L., and Stone, M. J. (2000) Characterization of binding between the chemokine eotaxin and peptides derived from the chemokine receptor CCR3. *J. Biol. Chem. 275*, 27250–27257.
47. Ye, J., Mayer, K. L., Mayer, M. R., and Stone, M. J. (2001) NMR solution structure and backbone dynamics of the CC chemokine eotaxin-3. *Biochemistry 40*, 7820–7831.
48. Mayer, K. L., and Stone, M. J. (2000) NMR solution structure and receptor peptide binding of the CC chemokine eotaxin-2. *Biochemistry 39*, 8382–8395.
49. Delaglio, F., Grzesiek, S., Vuister, G. W., Zhu, G., Pfeifer, J., and Bax, A. (1995) NMRPipe: A multidimensional spectral processing system based on UNIX pipes. *J. Biomol. NMR 6*, 277–293.
50. Crump, M. P., Rajarathnam, K., Kim, K. S., Clark-Lewis, I., and Sykes, B. D. (1998) Solution structure of eotaxin, a chemokine that selectively recruits eosinophils in allergic inflammation. *J. Biol. Chem. 273*, 22471–22479.
51. Ye, J., Mayer, K. L., and Stone, M. J. (1999) Backbone dynamics of the human CC-chemokine eotaxin. *J. Biomol. NMR 15*, 115–124.
52. Kay, L. E., Keifer, P., and Saarinen, T. (1992) Pure absorption gradient enhanced heteronuclear single quantum correlation spectroscopy with improved sensitivity. *J. Am. Chem. Soc. 114*, 10663–10665.
53. Parody, T. R., and Stone, M. J. (2004) High level expression, activation, and antagonism of CC chemokine receptors CCR2 and CCR3 in Chinese hamster ovary cells. *Cytokine 27*, 38–46.
54. Clubb, R. T., Omichinski, J. G., Clore, G. M., and Gronenborn, A. M. (1994) Mapping the binding surface of interleukin-8 complexes with an N-terminal fragment of the type 1 human interleukin-8 receptor. *FEBS Lett. 338*, 93–97.
55. Skelton, N. J., Quan, C., Reilly, D., and Lowman, H. (1999) Structure of a CXC chemokine-receptor fragment in complex with interleukin-8. *Structure 7*, 157–168.
56. Ravindran, A., Joseph, P. R., and Rajarathnam, K. (2009) Structural basis for differential binding of the interleukin-8 monomer and dimer to the CXCR1 N-domain: Role of coupled interactions and dynamics. *Biochemistry 48*, 8795–8805.
57. Wu, B., Chien, E. Y., Mol, C. D., Fenalti, G., Liu, W., Katritch, V., Abagyan, R., Brooun, A., Wells, P., Bi, F. C., Hamel, D. J., Kuhn, P., Handel, T. M., Cherezov, V., and Stevens, R. C. (2010) Structures of the CXCR4 chemokine GPCR with small-molecule and cyclic peptide antagonists. *Science 330*, 1066–1071.